Proposal of Limit Moment Equation Applicable to Planar/Non-Planar Flaw in Wall Thinned Pipes under Bending

メタデータ	言語: English
	出版者:
	公開日: 2011-10-04
	キーワード (Ja):
	キーワード (En):
	作成者: TSUJI, Masataka, MESHII, Toshiyuki
	メールアドレス:
	所属:
URL	http://hdl.handle.net/10098/4168

Proposal of Limit Moment Equation Applicable to Planar/Non-Planar Flaw

in Wall Thinned Pipes under Bending

Masataka TSUJI [a]*, Toshiyuki MESHII [b]

[a] Graduate Student, University of Fukui, 3-9-1 Bunkyo, Fukui, Fukui, JAPAN.

[b] Professor, Graduate School of Engineering, University of Fukui, 3-9-1 Bunkyo, Fukui, Fukui, JAPAN.

*Correspondent, E-mail: tsuji-m@u-fukui.ac.jp, FAX : +81-776-27-9764

Abstract

In this paper, a limit bending moment equation applicable to all types of planar and non-planar flaws in wall-thinned straight pipes under bending was proposed. A system to rationally classify the planar/non-planar flaws in wall-thinned pipes was suggested based on experimental observations focused on the fracture mode. The results demonstrate the importance of distinguishing between axial and circumferential long flaws in wall-thinned pipes.

Key words: limit moment, limit moment equation, bending, wall-thinned pipes, experimental stress analysis, fracture mode, fracture criterion, size effect

1. Introduction

Pipes in service experience local wall thinning due to corrosion, mechanical damage and other causes. Currently, much research is being conducted to establish and improve the safety assessment of pipes with local wall thinning (Janelle, 2005; Wilkowski et al., 2000). For pipes with local wall thinning that are both under pressure (Ahn et al., 2002; API/ASME, 2007; Kamaya et al., 2008a,b; Kim and Park, 2003a,b; Hasegawa et al., 2011) as well as a bending moment (Han et al., 1999; Kim and Park, 2003a,b; Shen and Zheng, 2004; Shim et al., 2004; Zheng et al., 2004), the fracture behavior (Ahn et al., 2002; Miyazaki et al., 1999; Takahashi et al., 2007; Tsuji and Meshii, 2011) and a safety assessment have been established and modified by the finite element method and through experiment.

For the case of evaluating the limit moment of wall-thinned straight pipes for a circumferential crack inside a cylinder (Fig. 1, top), a limit moment equation such as Kanninen's equation (Kanninen et al., 1982) is widely used (ANSI/ASME B31.G, 1991). This engineering judgment is justified because the limit moment of a crack (planar flaw) will likely give a conservative estimate for flaws (non-planar flaws) in wall-thinned pipes. However, it should not be overlooked that the following implicit limitations exist when applying the equation for a crack to non-planar flaws.

1) The fracture mode of the non-planar flaw under consideration is identical to that of the crack.

2) The effect of the axial length δ_z of the non-planar flaw (Fig. 1, middle and bottom) on the limit moment M_c, which is not considered for a circumferential crack, is small or negligible.

1

Regarding the fracture mode in the first limitation, Miyazaki et al. (Miyazaki et al., 1999) pointed out in their experimental study that the fracture mode of wall-thinned pipes is not always collapsed (ovalization), and cracking can be observed for a specific combination of flaw configurations (Fig. 1, t_1 and θ). Note that their study was made for a constant axial flaw length δ_z without an internal pressure. Thus, the examination of the effect of the axial length of wall thinning (Fig. 1, δ_z) on the fracture mode is not necessarily sufficient.

The effect of δ_z on M_c in the second limitation has been examined by Han (Han et al., 1999), Zheng (Zheng et al., 2004) and Kim et al. (Kim et al., 2006). They created a limit-load analysis and obtained similar results showing that a) M_c monotonically decreases with increases in δ_z, and b) M_c converges to a flaw with a length of $\delta_z/(R_m\,t)^{0.5} > 1.5$ (R_m: radius of the pipe, t: wall thickness). If we accept these two findings, M_c for a crack (i.e., $\delta_z = 0$) is larger than that for a non-planar flaw (wall thinning), and as a result, using the crack equation for a non-planar flaw would be non-conservative. This curious finding might be a result of assuming that the fracture mode is always collapsed.

Therefore, in this work, attention is focused on the two implicit assumptions listed and examined the effects that δ_z has on the fracture mode and the limit bending moment M_c. Using concrete, systematic tests of carbon steel pipes were conducted with artificial wall-thinned flaws under a combined pressure and bending load to propose an application guideline for applying a limit moment equation for a circumferential crack inside a cylinder (Fig. 1 top) to non-planar flaws in wall-thinned pipes (Fig. 1,

middle and bottom). Based on the test results, a system to rationally classify planar/non-planar flaws in wall-thinned pipes was proposed, and finally, a limit moment equation applicable to both planar/non-planar flaws in wall-thinned straight pipes was created. As a first step, flaws with a size of $\theta \leq \pi$ and subjected to tensile stresses were examined.

2. Experiment

It was considered that Han's curious result (i.e., M_c monotonously increases as $\delta_z \rightarrow 0$) occurred because they assumed that the fracture mode was always in a collapsed state for all the flaw configurations. However, it was not clear from Miyazaki et al.'s experimental result whether the fracture mode changed from collapsed to cracking as $\delta_z \rightarrow 0$ because their experiment was limited to the case of a constant δ_z. Thus, in this work, the goal was to experimentally verify that:

- The fracture mode changes from a collapsed state to cracking for small δ_z.

- The effect of δ_z on M_c is not negligible.

- M_c decreases as $\delta_z \rightarrow 0$, and thus, applying the crack equation to non-planar flaw is conservative.

2.1 Specimen

The test specimen configuration is shown in Fig. 2. Because the current Japanese regulation on the wall-thinned pipe is based on the minimum wall thickness, the actual flaw was modeled as a constant depth rectangular flaw as shown in Fig. 3, and a limit load equation for this model was proposed. The dimensions of the artificial flaw of each specimen and the limit moment M_c obtained from each test are summarized in Table 1. The edge of the square flaw was tapered to avoid stress concentration and to

3

secure conservatism in the experimental result. The design values of the nominal and minimum wall thicknesses was set to $t = 4$ mm and $t_{min} = 2$ mm for all specimens, so the model often found that $t_{min}/t = 0.5$ for pipes in nuclear power plants. The ligament of the flaw t_1 was set equal to the t_{min} for all of the cases. $t_{1Measured}$, which is defined as the measured ligament wall thickness, is also listed in Table 1. The slashed columns for $t_{1Measured}$ indicate that the ligament thickness measurement was difficult for this groove type flaw.

The specimen material was carbon steel JIS (Japanese Industrial Standards) STPT 370. The chemical compositions and the tensile strengths of the specimen are shown in Tables 2 and 3, respectively. Here, σ_B, σ_{YS}, σ_f and ε_B are the tensile stress, the yield stress, the flow stress and the elongation, respectively. σ_f was defined as an average of σ_B and σ_{YS}.

Note that all of the tests were conducted at room temperature. The pressure applied given by $p = p_{max} = 6.4$ MPa was selected as the maximum rated pressure that corresponds to the t_{min} calculated based on JSME S NC1-2008.

2.2 Test system

The four-point bending test system is shown in Fig. 4. In the tests, the internal pressure p was first applied to a rated pressure of p_{max}, and then the load W was applied gradually until a maximum load W_c was reached. Here, the limit moment is $M_c = W_c b/2 = 0.1525 W_c$ kNm, and the maximum load W_c was defined as the two-second average around the observed maximum value measured with 0.01 second

4

intervals.

3. Test results

3.1 Fracture mode

The fracture mode of the wall-thinned pipes of 80A and $t_1/t = 0.5$ is summarized in Fig. 5. It can be

seen from the figure that although the ligament thickness of the artificial flaw t_1 was kept constant for this

study (different from Miyazaki et al.'s work (Miyazaki et al., 1999)), cracking was generally observed for

a large circumferential flaw angle θ and a small flaw axial length δ_z. It is interesting that cracking was

observed for the case in which δ_z was as large as 20 mm and could not be considered as a circumferential

groove in a general sense. In summary, the test results showed that for a case where $t_1/t = 0.5$, the fracture

mode changed from collapsed to cracking when $\delta_z/(\theta R_m) \leq 0.25$.

Note that not only do the planar dimensions of the flaw (δ_z, θ) affect the fracture mode, but the

ligament thickness t_1 affects the fracture mode as well (Miyazaki et al., 1999).

It can be concluded from the above examinations of the fracture mode that non-planar flaws such as

those for the case of 80A, $\delta_z = 20$ mm, $\theta = \pi$, and $t_1/t = 0.5$ can experience circumferential cracking, and

therefore engineers should not assume collapse as a failure criterion for all types of non-planar flaws

found in wall-thinned pipes. This is especially true for flaws with a relatively small δ_z.

3.2 Effect of the flaw configuration on the limit moment

Next, the effect of the axial length of the non-planar flaw δ_z on the limit moment, which is not

considered for a circumferential crack, was examined. For this purpose, the limit moment obtained from

our experiment M_c and that predicted by the following Kanninen's equation M_{cK} (Kanninen et al., 1982)

was compared in Fig. 6 for a flaw aspect ratio $\delta_z/(\theta R_m)$. It is thought that the ratio M_c/M_{cK} expresses the

discrepancy in a model of circumferential crack.

- $(\theta/2 + \beta) < \pi$

$$M_{cK} = M_0\left[\sin\beta - \frac{t-t_1}{2t}\sin\frac{\theta}{2}\right] \tag{1}$$

$$\beta = \frac{\pi}{2}\left[1 - \frac{t-t_1}{\pi t}\frac{\theta}{2} - \frac{P}{2\pi R_m t\sigma_f}\right] \tag{2}$$

- $(\theta/2 + \beta) > \pi$

$$M_{cK} = M_0\left[\frac{t_1}{t}\sin\beta + \frac{t-t_1}{2t}\sin\frac{\theta}{2}\right] \tag{3}$$

$$\beta = \frac{\pi t}{2t_1}\left[2\frac{t_1}{t} + \frac{t-t_1}{\pi t}\frac{\theta}{2} - 1 - \frac{P}{2\pi R_m t\sigma_f}\right] \tag{4}$$

Here, the nominal dimensions of the flaw-less cylinder are R_m: the mean radius of pipe and t: the wall

thickness, and the flaw dimensions are t_1: the ligament thickness, θ: the circumferential angle and δ_z: the

axial length. $P \ (= p\pi r_i^2)$ is the axial load, p is the internal pressure, r_i is the inner radius of pipe and $M_0 \ (=$

$4\sigma_f R_m^2 t)$ is the limit moment of the flaw-less cylinder.

It can be seen from Fig. 6 that the effect of δ_z on the limit bending load M_c is not negligible. It can

also be observed from the figure that M_c monotonously decreases with the increase in δ_z for a flaw aspect

of $\delta_z/(\theta R_m) > 0.25$ that corresponds to the fracture mode of collapse. This tendency coincides with that

predicted by Han's limit load analysis (Han et al., 1999), which assumed that the fracture mode was

collapse. On the other hand, in the case of $\delta_z/(\theta R_m) \leq 0.25$, which corresponds to fracture mode of

cracking, M_c monotonously increased due to an increase in δ_z. This tendency is inconsistent with what

Han predicted, but satisfactory based on the point that M_c for a crack ($\delta_z = 0$) is smaller than that of a

non-planar flaw, and thus applying the crack equation to a non-planar flaw is conservative. However, it

can also be seen from Fig. 6 that the conservatism of applying the crack equation to a non-planar flaw is

as small as 20% for a flaw with $\delta_z/(\theta R_m) > 1.0$, i.e., a square or an axially long flaw.

4. Proposal of a limit moment equation applicable to a planar/non-planar flaw in wall-thinned pipes

In summary,

– The effect of δ_z on the limit moment M_c is not negligible and should be properly reflected in the

limit moment equation.

– The effect of δ_z on the limit moment M_c is different for the fracture mode, and the fracture mode

should be properly reflected in the limit moment equation.

– The fracture mode can be predicted by the flaw aspect ratio $\delta_z/(\theta R_m)$. Cracking occurs for $\delta_z/(\theta R_m)$

≤ 0.25, and collapse occurs for $\delta_z/(\theta R_m) > 0.25$.

Thus, we propose that the limit moment equation is applicable to planar and non-planar flaws of $0 \leq$

$\theta \leq \pi$ in wall-thinned pipes as follows:

$$M_{cFU} = 4\sigma_f R_m^2 t_1 \cdot g\left(\Theta = \frac{\theta}{2\pi}, \Delta = \frac{\delta_z}{\sqrt{R_m t}}\right) \qquad (5)$$

$$(0 \leq \theta \leq \pi)$$

The shape function g was defined as follows, and its concrete function coefficients a_i and b_j are given for each flaw aspect ratio $\delta_z/(\theta R_m)$ range in Eqs. (7) and (8). This shape function was derived in two steps: First, by fitting the experimental data M_c for $\Theta = 0.5$ and 0.005 (both 80A and $t_1/t = 0.5$). We used least squares method and made approximate functions of $g = M_c/M_1$ ($M_1 = 4\sigma_f R_m^2 t_1$) about maximum and minimum Θ, and then, these two equations were linearly interpolated for Θ. Here, $\Theta = 0.005$ represents a case for an axial crack. The limit moment equation was classified $\delta_z/(\theta R_m) \leq 0.25$ and $\delta_z/(\theta R_m) > 0.25$.

$$g\left(\Theta = \frac{\theta}{2\pi}, \Delta = \frac{\delta_z}{\sqrt{R_m t}}\right) = \left(\sum_{i=0}^{1} a_i \Theta^i\right) \cdot \left(\sum_{j=0}^{3} b_j \Delta^j\right) \tag{6}$$

where,

- $\delta_z/(\theta R_m) \leq 0.25$

$$g = 1.275 + 0.48426\Delta - 0.147849\Delta^2 + 0.00840024\Delta^3$$
$$+ (-0.7885 + 0.48426\Delta - 0.147849\Delta^2 + 0.00840024\Delta^3)(2\Theta - 1) \tag{7}$$

- $0.25 < \delta_z/(\theta R_m)$

$$g = 1.9633 - 0.135608\Delta + 0.0119421\Delta^2 - 0.000350552\Delta^3$$
$$+ (-0.100201 - 0.135608\Delta + 0.0119421\Delta^2 + 0.000350552\Delta^3)(2\Theta - 1) \tag{8}$$

Note that the limit moment equation was compiled in the form of the fundamental strength based on the ligament wall thickness multiplied by the shape function. This style was chosen because Japanese regulations for wall-thinned pipes are based on the minimum required wall thickness t_{min} determined by the construction code.

5. Discussion

The test results of the limit moment M_c were compared with those predicted by our equation M_{cFU} in

8

Fig. 7 in the form of M_c/M_{cFU}. In this figure, the values for M_c/M_{cK} were also plotted for reference, where

M_{cK} is Kanninen's equation defined by Eqs. (1) and (3). The markers with () show that the design

ligament thickness t_1 was used instead of the measured thickness $t_{1Measured}$ for these plots because the

accurate ligament thickness measurement was difficult for these groove-like flaws.

It is seen from Fig. 7 that our equation M_{cFU} gives an accurate estimate of the experimental results

regardless of the flaw aspect ratio. On the other hand, the conservatism of Kanninen's equation, which is

an equation for a crack and expected to give sufficient conservatism, varied in its flaw aspect ratio. For

example, Kanninen's equation was very conservative for the flaw of $\delta_z/(\theta R_m) \fallingdotseq 0.25$, but when the flaw

became square or rectangular ($\delta_z/(\theta R_m) \geq 1.0$), the conservatism was unexpectedly as small as 20%.

It may be thought that conservative estimation is most often used to ensure the safety of nuclear

power plants, and thus, applying a crack equation to a non-planar flaw is satisfactory. As a result, a new

limit moment equation is not necessary. However, it should not be forgotten that one of the motivations

behind recent research projects is to reduce the overconservatism in applying a crack equation to

non-planar flaws found in wall-thinned pipes. Because M_c/M_{cFU} was very close to unity regardless of the

flaw configuration, applying the proposed equation M_{cFU} will certainly contribute to reducing

overconservatism.

In the introduction, it was noted that the effect of δ_z on M_c has been examined by Han et al. (Han et

al., 1999), and their limit-load analysis result showed that M_c monotonically decreases with an increase in

δ_z, and M_c converges to a flaw with a length of $\delta_z/(R_m\ t)^{0.5} > 1.5$. To directly compare our experimental results with Han's analytical ones, Fig. 6 was re-compiled in the form of Fig. 8 with Han's result for the case of $\theta/2\pi = 1/2$ and $t_1/t = 0.5$.

We see from Fig. 8 that for the case in which the fracture mode was cracking, M_c monotonously increased due to an increase in δ_z. This tendency is inconsistent with what Han predicted, but satisfactory in that M_c for a crack ($\delta_z = 0$) is smaller than that of a non-planar flaw, and thus applying crack model to a non-planar flaw is conservative. Therefore, we emphasize again the importance of considering the fracture mode in evaluating the limit moment of flaws in wall-thinned cylinders.

It can also be seen from Fig. 8 that M_c did not saturate for a long flaw of $\delta_z/(R_m\ t)^{0.5} > 1.5$. For example, when $\theta/2\pi = 1/2$, M_c for a flaw of $\delta_z/(R_m t)^{0.5} > 11.5$ was approximately equal to that of $\delta_z/(R_m\ t)^{0.5} \approx 0.1$. This result demonstrates that applying a limit moment equation for a crack to a non-planar flaw has very little conservatism for axially long flaws. The discrepancy found between our experimental results and Han's analytical ones for axially long flaws is an issue to be solved in the future because this discrepancy cannot be explained by the fracture mode issue.

It should be noted that the internal pressure was not considered in the proposed limit moment equation (5). This is because the equation was intended to be applied to the pipes that were designed under the Japanese nuclear power plant construction code (JSME S NC1-2008). In concrete, the minimum wall thickness t_{min} was selected for the rated maximum pressure p_{max} operating under this rated

10

pressure, and the wall thinning is regulated so that the minimum wall thickness is ensured. This means

that t_{min} is basically selected so that the hoop stress by the thin wall cylinder theory becomes lower than

the yield stress σ_{YS}.

$$t_{min} \fallingdotseq p \frac{R_m}{\sigma_{YS}} \qquad (9)$$

If the effect of the internal pressure p on the limit moment is evaluated by Kanninen's equation (1), this

effect is considered through β in equation (2). Considering the fact that t_{min}/t is usually set as 0.5 in

nuclear power plants and by setting the axial force $P = p\pi r_i^2$ (r_i: inner radius) in Eq. (9),

$$\beta = \frac{1}{2}\left\{\pi - \left(1 - \frac{t_1}{t}\right)\theta\right\} - \frac{\pi}{32}\frac{\sigma_{YS}}{\sigma_f}\left(-2 + \frac{t}{R_m}\right)^2 \qquad (10)$$

is deduced. From this equation, it can be seen that the effect of the internal pressure p on the limit

moment M_{cK} has disappeared. Thus, it was assumed that the effect of p on the limit moment was

secondary and p was not considered as a parameter in our limit moment equation. We will consider the

effect of p by analysis in the future.

6. Conclusion

In this paper, the four-point bending test was performed and the effect that δ_z has on the fracture mode

and the limit bending moment M_c was examined. Regarding the fracture mode, it was confirmed that the

effect of δ_z on M_c was not negligible, which was not clear in Miyazaki et al.'s research. Regarding the

effect of δ_z on the limit bending moment M_c, it was confirmed that M_c decreases as $\delta_z \rightarrow 0$, which was

different from Han et al.'s research, but satisfactory based on the premise that applying a crack equation

11

to a non-planar flaw was conservative. A system to rationally classify planar/non-planar flaws in

wall-thinned pipes was also proposed based on the experimental observations witnessed on the fracture

mode. Finally, a limit moment equation applicable to planar/non-planar flaws with $0 \leq \theta \leq \pi$ found in

wall-thinned straight pipes was proposed.

Acknowledgement

List of Tables

Table 1 Dimensions of the artificial flaws

$\theta/2\pi$	$t_{1\text{Measured}}$ (mm)	δ_z (mm)	$\dfrac{\delta_z}{\sqrt{R_m t}}$	$\delta_z/(\theta R_m)$	M_c^{Exp} (kNm)	Specimen no.	Specimen type in Fig. 3
1/2	2.08	140	11.36	1.173	6.85	10-03	(a)
1/2	2.18	107	8.68	0.896	7.21	09-04	(a)
1/2	2.10	37	3.00	0.310	7.67	09-03	(a)
1/2	1.96	20	1.62	0.168	7.51	10-04	(a)
1/2	–	1	0.08	0.008	6.86	09-01	(c)
1/3	2.08	107	8.68	1.344	7.52	10-05	(a)
1/3	1.95	20	1.62	0.251	8.31	10-07	(a)
1/3	2.04	10	0.81	0.126	8.46	10-08	(a)
1/3	1.96	1	0.08	0.013	6.68	10-15	(c)
1/6	2.09	74	6.00	1.860	8.62	10-11	(a)
1/6	2.04	40	3.24	1.005	8.75	10-12	(a)
1/6	2.00	10	0.81	0.251	8.81	10-13	(a)
1/6	1.97	6	0.49	0.151	8.70	10-14	(a)
1/6	2.05	1	0.08	0.025	8.10	10-16	(c)
1/20	2.11	12	0.97	1.005	9.73	10-10	(a)
1/20	2.08	6	0.49	0.503	9.40	10-19	(b)
1/200	2.03	20	1.62	16.75	9.56	10-17	(b)
1/200	2.04	10	0.81	8.377	9.24	10-18	(b)

Table 2 Chemical compositions of the specimen

		C	Si	Mn	P	S
STPT370	Specified	< 0.25	0.10–0.35	0.30–0.90	< 0.035	< 0.035
STPT370	Measured	0.21	0.23	0.48	0.008	0.004

Table 3 Tensile strengths of the specimen

		σ_{YS} (MPa)	σ_B (MPa)	σ_f (MPa)	ε_B
STPT370	Specified	> 215	> 370	–	> 0.30
STPT370	Measured	301	463	382	0.39

List of Figures

15

References

ANSI/ASME B31.G., 1991. Manual for Determining the Remaining Strength of Corroded Pipelines.

API/ASME, 2007. Fitness-For-Service API 579/ASME FFS-1-2007.

Ahn, S.-H., Nam, K.-W., Yoo, Y.-S., Ando, K., Ji, S.-H., Ishiwata, M., Hasegawa, K., 2002. Fracture behavior of straight pipe and elbow with local wall thinning. Nuclear Engineering and Design 211, 91-103.

Han, L.-h., He, S.-y., Wang, Y.-p., Liu, C.-d., 1999. Limit moment of local wall thinning in pipe under bending. International Journal of Pressure Vessels and Piping 76, 539-542.

Hasegawa, K., Meshii, T., Scarth, D. A., 2011. Assessment of piping field failures and burst tests on carbon steel pipes with local wall thinning using ASME section XI code case N-597-2. Transactions of ASME, Journal of Pressure Vessel Technology. 133, 031101-1-10.

JSME S NC1-2008, 2008. Code for nuclear power generation facilities – rules on fitness for service for nuclear power plants. 1. The Japan Society of Mechanical Engineers.

Janelle, J.L., 2005. An overview and validation of the fitness-for-service assessment procedures for local thin areas. The University of Akron.

Kamaya, M., Suzuki, T., Meshii, T., 2008a. Failure pressure of straight pipe with wall thinning under internal pressure. International Journal of Pressure Vessels and Piping 85, 628-634.

Kamaya, M., Suzuki, T., Meshii, T., 2008b. Normalizing the influence of flaw length on failure pressure of straight pipe with wall-thinning. Nuclear Engineering and Design 238, 8-15.

Kanninen, M., Zahoor, A., Wilkowski, G., Abousayed, I., Marschall, C., Broek, D., Sampath, S., Rhee, H., Ahmad, J., 1982. Instability predictions for circumferentially cracked Type-304 stainless steel pipes under dynamic loading. EPRI Report Number NP-2347, April.

Kim, J.W., Park, C.Y., 2003a. Criterion for failure of internally wall thinned pipe under a combined pressure and bending moment. In: Transactions of the 17th International Conference on Structural Mechanics in Reactor Technology (SMIRT 17), Prague, August, Paper G07-5 (2003), p. 8.

Kim, J.W., Park, C.Y., 2003b. Effect of length of thinning area on the failure behavior of carbon steel pipe containing a defect of wall thinning. Nuclear Engineering and Design 220, 274-284.

Kim, Y.-J., Oh, C.-K., Park, C.-Y., Hasegawa, K., 2006. Net-section limit load approach for failure strength estimates of pipes with local wall thinning. International Journal of Pressure Vessels and Piping 83, 546-555.

Miyazaki, K., Kanno, S., Ishiwata, M., Hasegawa, K., Hwan Ahn, S., Ando, K., 1999. Fracture behavior of carbon steel pipe with local wall thinning subjected to bending load. Nuclear Engineering and Design 191, 195-204.

Takahashi, K., Ando, K., Hisatsune, M., Hasegawa, K., 2007. Failure behavior of carbon steel pipe with local wall thinning near orifice. Nuclear Engineering and Design 237, 335-341.

Tsuji, M., Meshii, T., 2011. Extending image processing strain measurement system to evaluate fracture behavior of wall-thinned pipes. Nuclear Engineering and Design in press DOI: 10.1016/j.nucengdes.2011.07.026.

Wilkowski, G., Stephens, D., Krishnaswamy, P., Leis, B., Rudland, D., 2000. Progress in development of acceptance

criteria for local thinned areas in pipe and piping components. Nuclear Engineering and Design 195, 149-169.

Zheng, M., Luo, J.H., Zhao, X.W., Zhou, G., Li, H.L., 2004. Modified expression for estimating the limit bending moment of local corroded pipeline. International Journal of Pressure Vessels and Piping 81, 725-729.

	crack	wall thinning
flaw depth	a	$t-t_1$
axial length	/	δ_z
circ. length	θ	θ
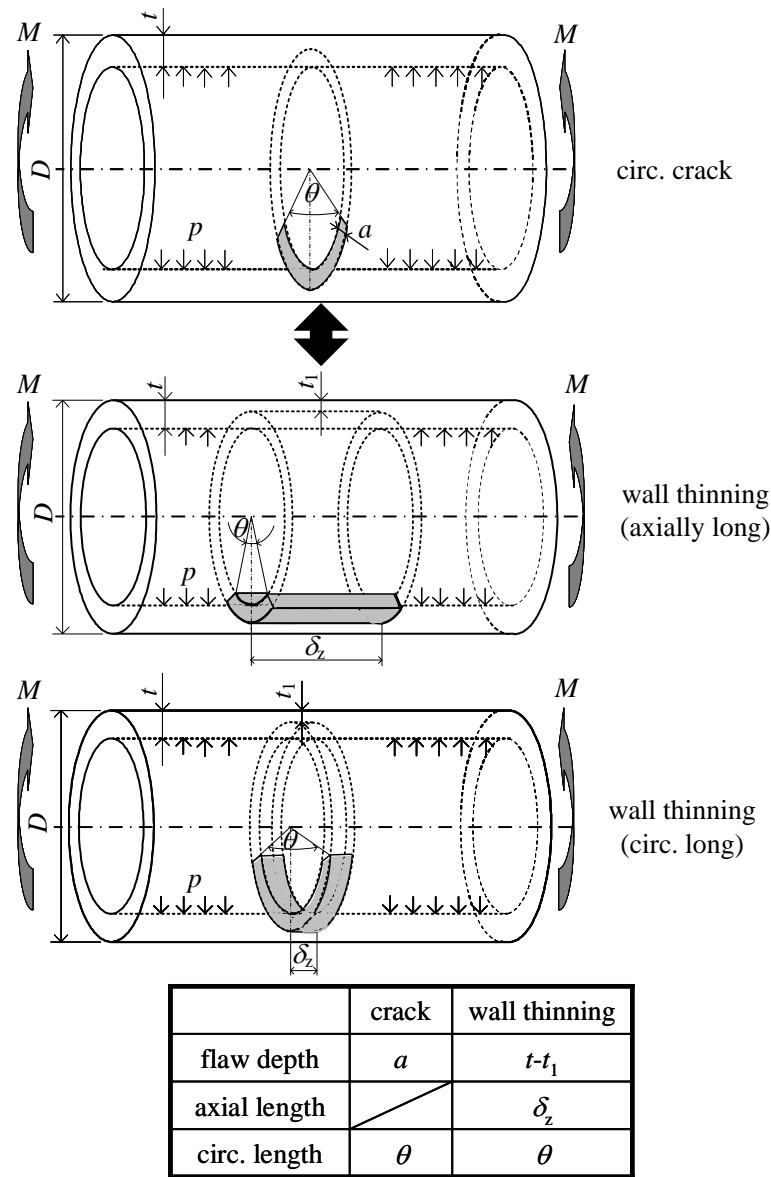
Fig. 1 Circumferential planar flaw and non-planar flaws
(axially and circumferentially long) in a cylinder
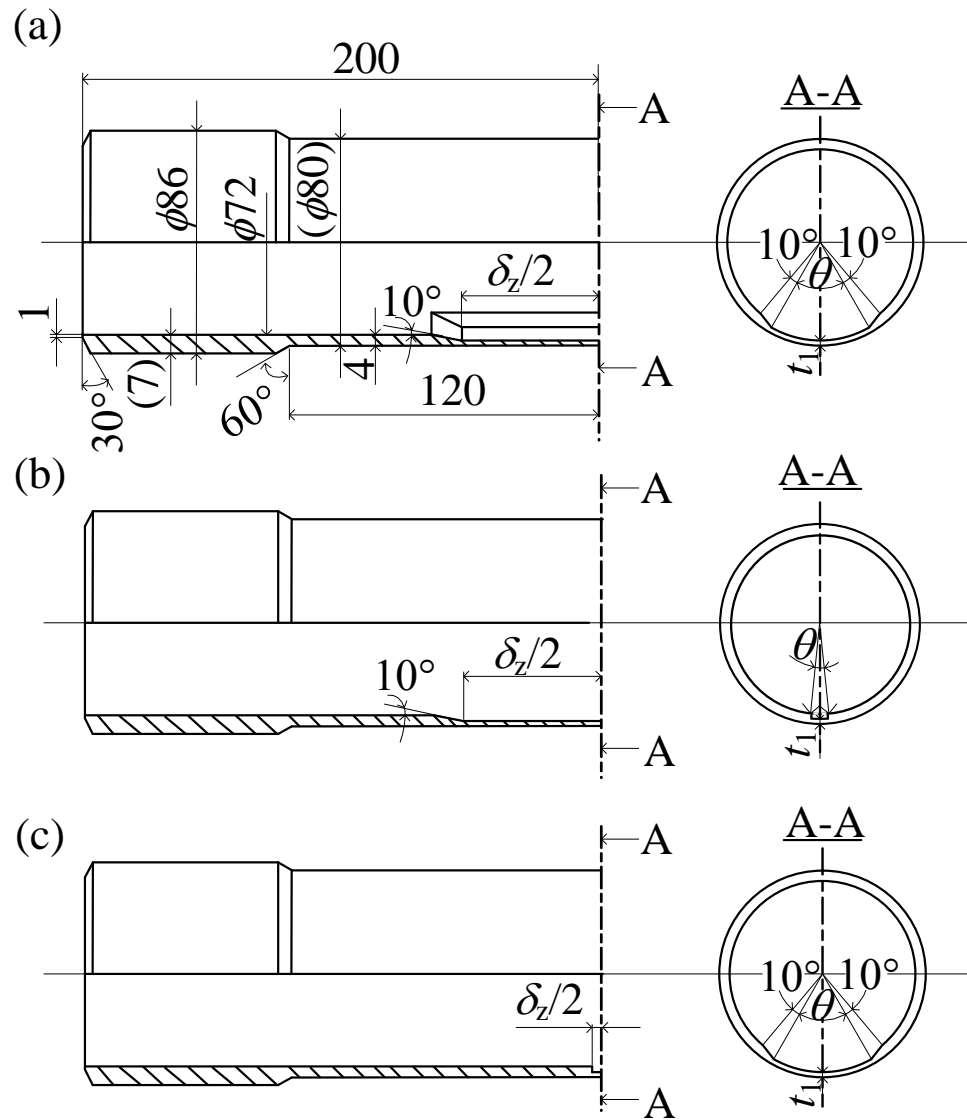
Fig. 2 Three different specimen types for bending test
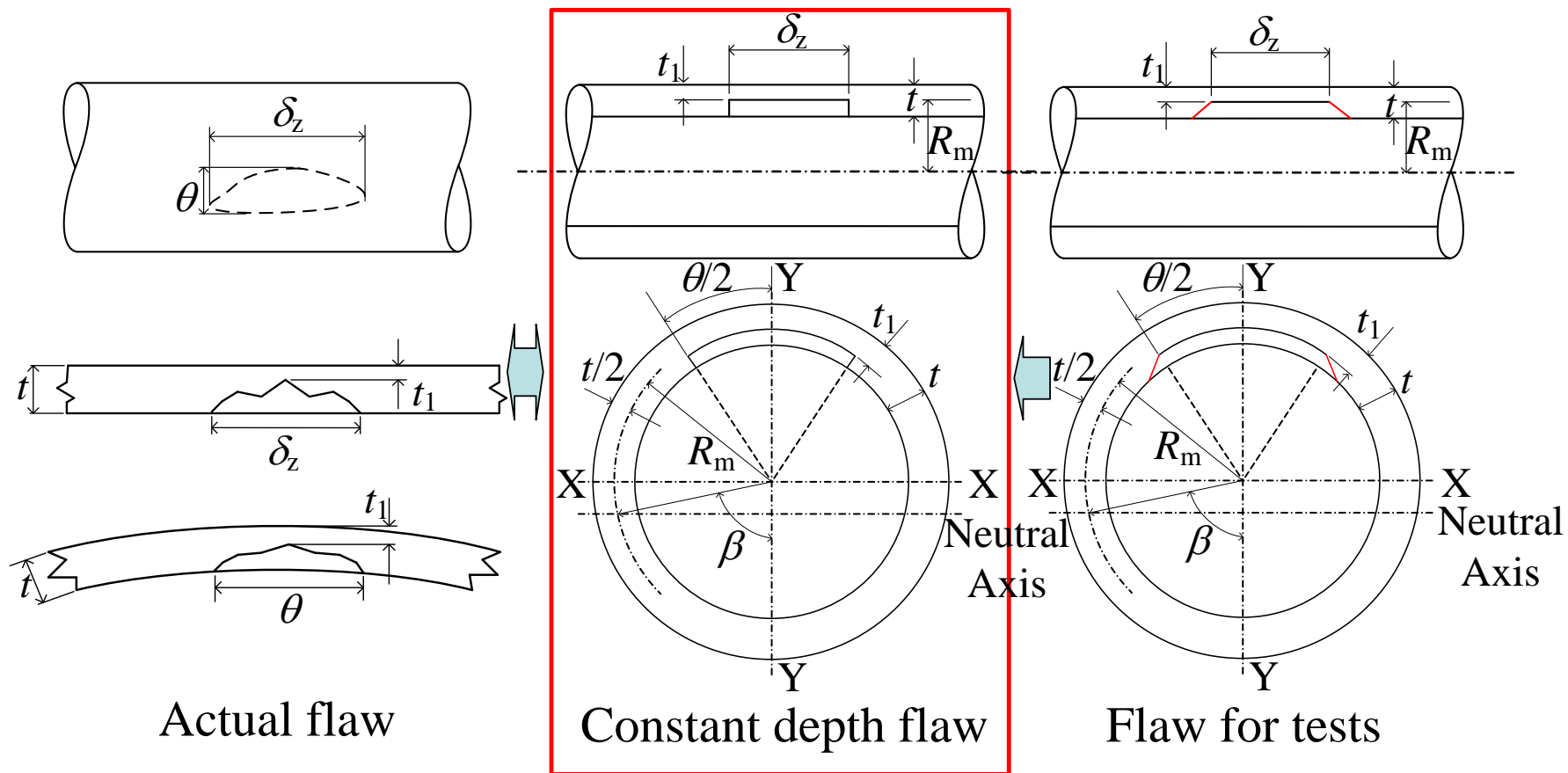
Fig. 3 Idealized flaw modelling for a constant depth rectangular flaw
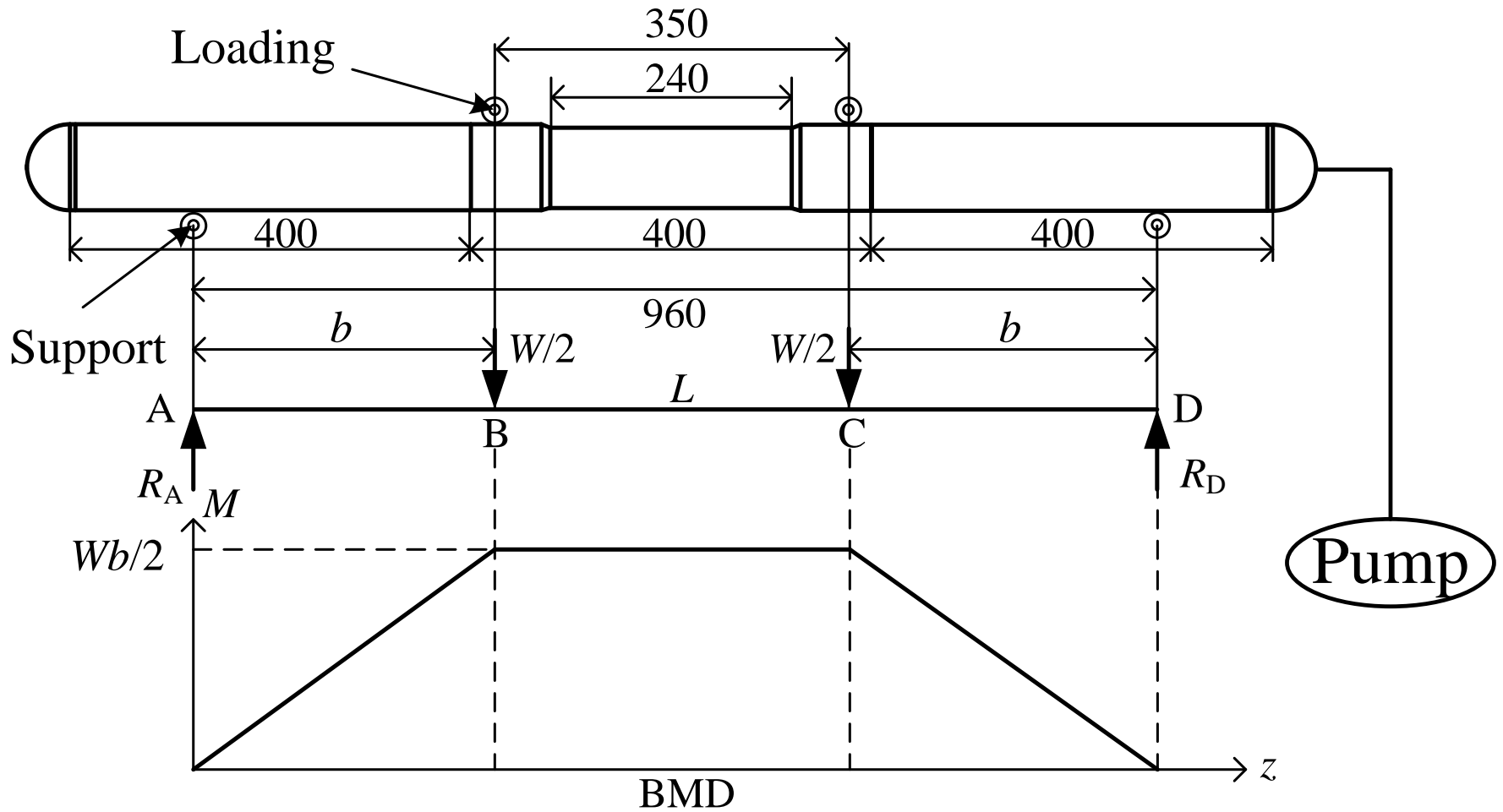
Fig. 4 Four-point bending test and bending moment diagram (unit: mm)

θ rad δ_z mm	$\pi/100$	$\pi/3$	$2\pi/3$	π
107	Collapse			
20				
10				
1				

$\delta_z/(\theta R_m) > 0.25$	$\delta_z/(\theta R_m) \leq 0.25$	Cracking
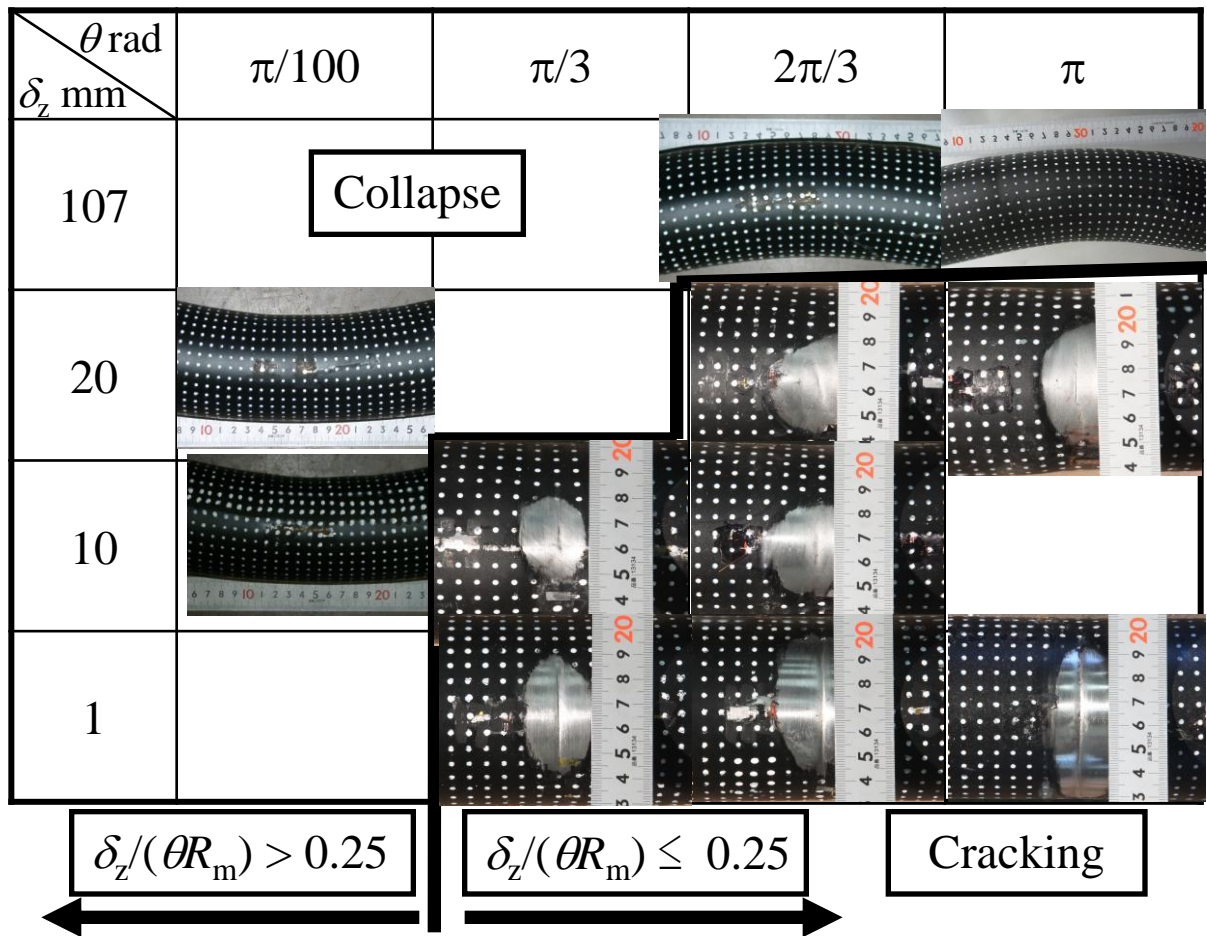
Fig. 5 Fracture mode under bending (80A, $t_1/t = 0.5$)
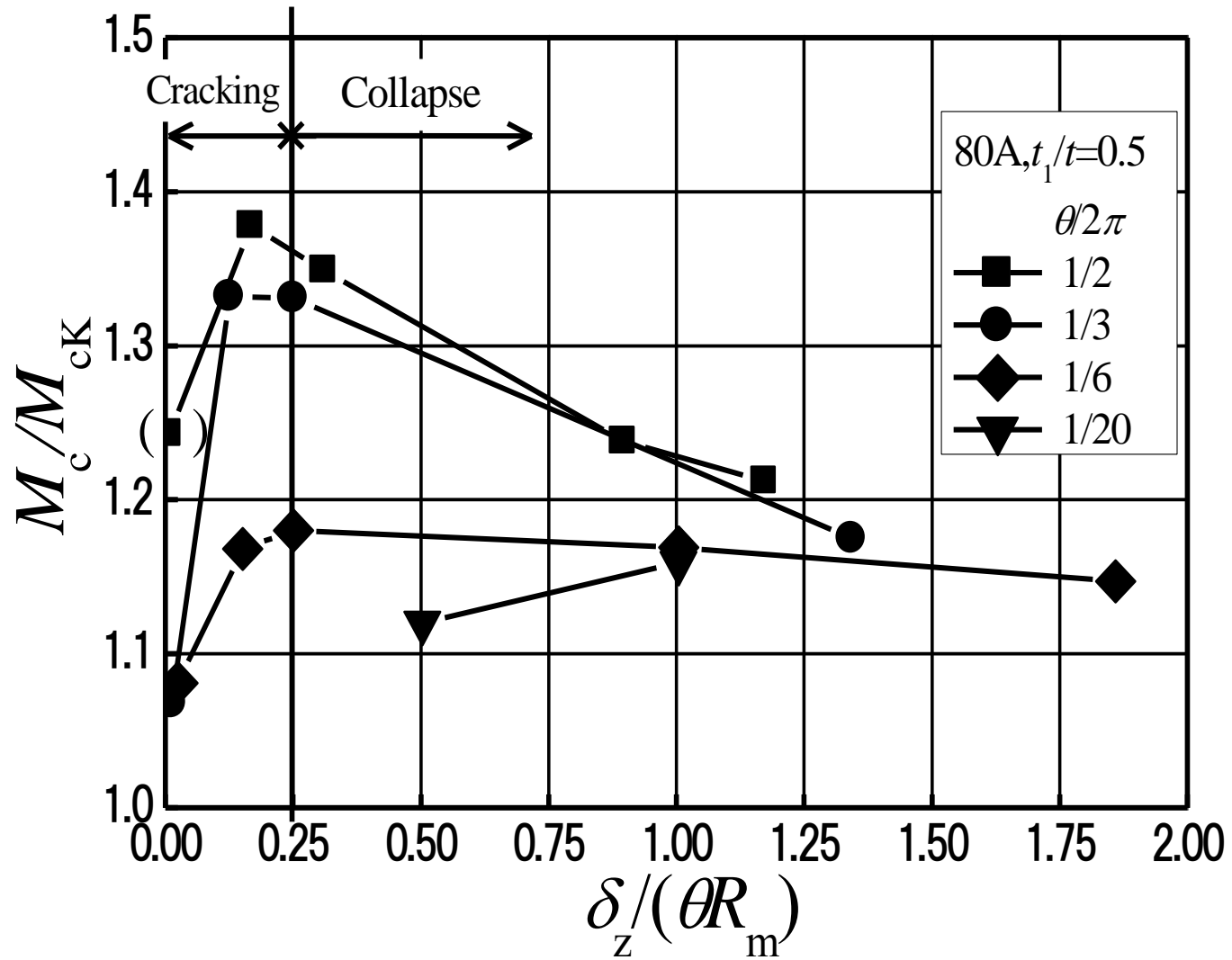
Fig. 6 Effect of flaw configuration on the limit moment in M_c/M_{cK} (80A, $t_1/t = 0.5$)
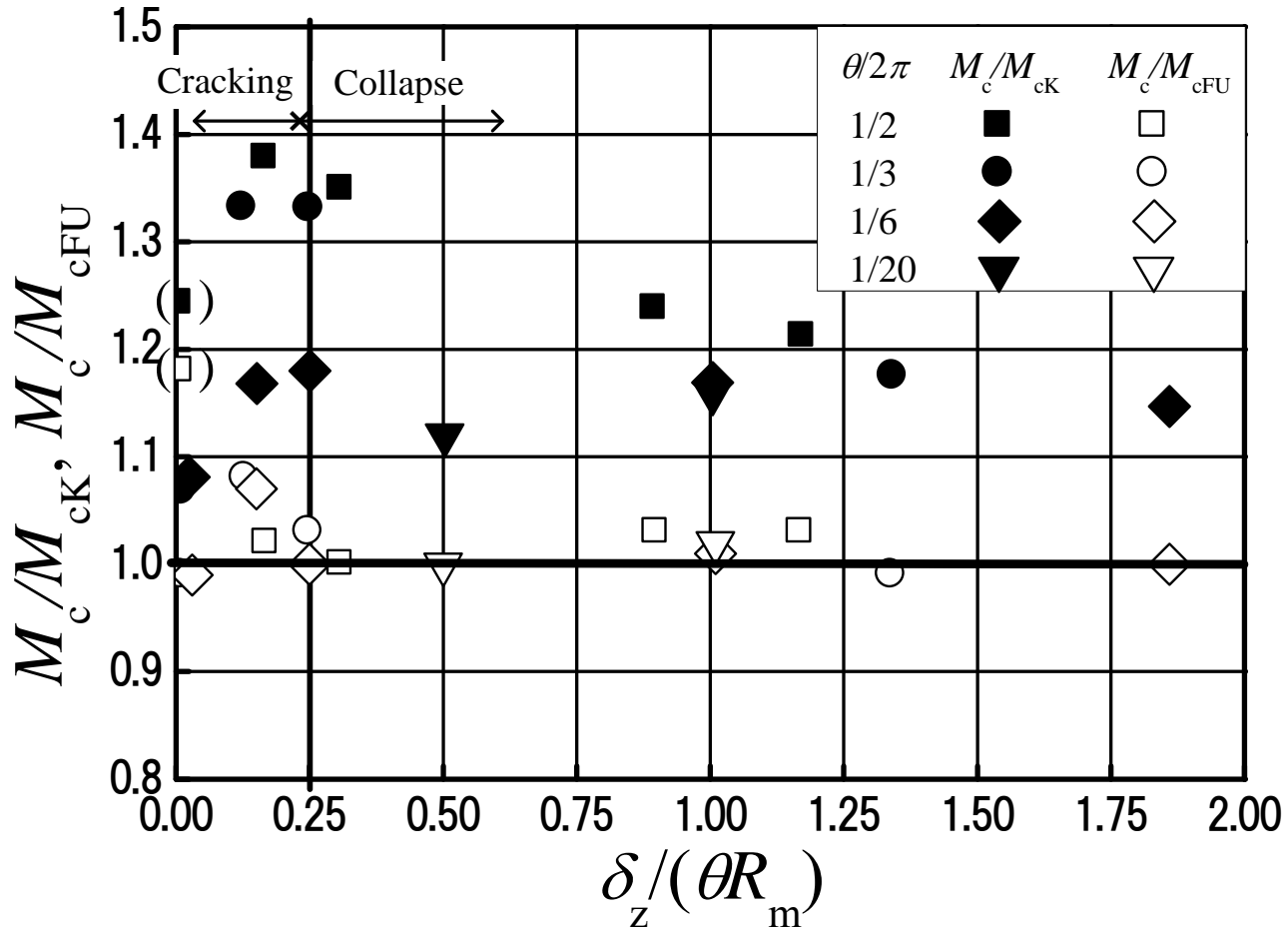
Fig. 7 Validity of the proposed equation (80A, $t_1/t = 0.5$; $0 \leq \delta_z/(\theta R_m) \leq 2$)
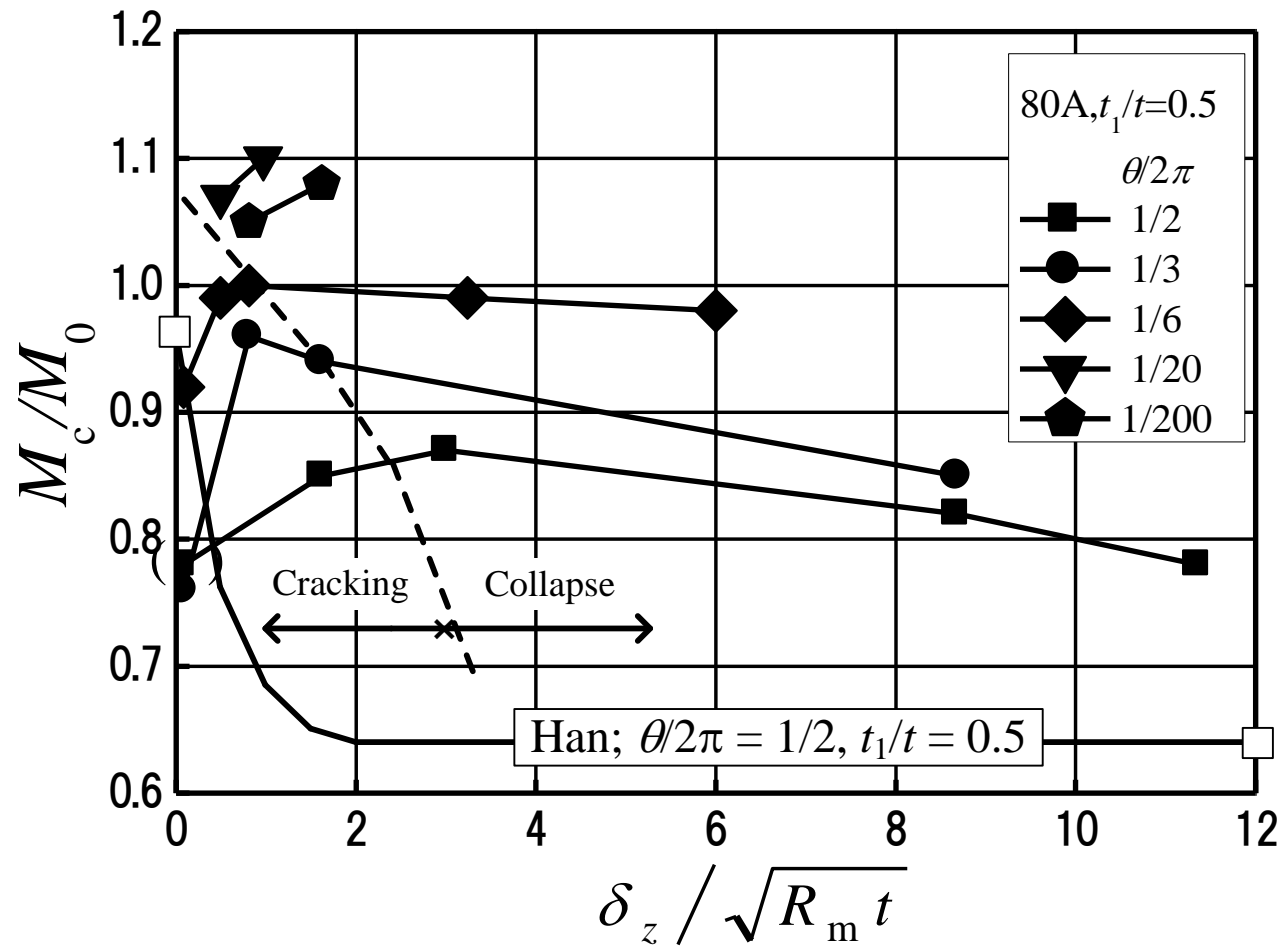
Fig. 8 Effect of flaw configuration on the limit moment in M_c/M_0 (80A, $t_1/t = 0.5$)